

THE TIME SECOND-ORDER CHARACTERISTIC FEM FOR NONLINEAR MULTICOMPONENT AEROSOL DYNAMIC EQUATIONS IN ENVIRONMENT

KAI FU, DONG LIANG*, WENQIA WANG, AND MING CUI

Abstract. An efficient time second-order characteristic finite element method for solving the nonlinear multi-component aerosol dynamic equations is developed. While a highly accurate characteristic method is used to treat the advection multi-component condensation/evaporation process, a time high-order extrapolation along the characteristics is applied to approximate the nonlinear multi-component coagulation terms. The scheme is of second order accuracy in time for the multi-component problems. We study the theoretical analysis and obtain the time second-order error estimate of the scheme. Numerical experiments are further given to confirm the theoretical results. The dynamic behaviours of multi-component aerosol distributions are also simulated for the multi-component aerosol problems of aerosol water, black carbon and sulfate components with different tri-modal log-normal initial distributions.

Key words. Multi-component aerosol dynamic equations, condensation/evaporation, nonlinear coagulation, characteristic method, characteristic extrapolation, error estimate.

1. Introduction

Global climate change and warming in atmosphere have been widely recognized. As one of most important constituents, aerosols are minutes particles suspended in atmosphere, which play an important role in climate change, atmospheric chemistry, and air pollution issues including visibility reduction and adverse human health effects. The research on the multi-component aerosol dynamics is of great importance, which can provide a better understanding of the distribution of aerosol particles in atmospheric environment and can further help to predict and protect the atmospheric environment. Modeling the composition and size distributions of atmospheric aerosols is very important as they determine the optical properties of particles, and moreover, the aerosol composition influences the ability of particles to act as cloud condensation nuclei or ice nuclei.

The evolution of the size distribution of aerosols is governed by the nonlinear aerosol dynamic equation, which describes the impacts of several processes such as condensation, coagulation, emission, and deposition, etc. Some numerical methods were developed, including sectional method [3, 7], moment method [5, 12], modal method [1, 16], stochastic approach [4], finite element method [13], etc. The sectional method is simple but usually leads to numerical diffusion when treating condensation/evaporation [7]. The modal method has high efficiency but has less physical representation of aerosol distributions and less accuracy. The moment method is not suitable for the simulation of multi-modal distributions. The drawback of the stochastic method is that it can not get a satisfied accuracy. Recently,

Received by the editors March 6, 14, and in revised form, November 11, 2014.

2000 *Mathematics Subject Classification.* 65M10, 65M15, 65N10, 65N15.

*Corresponding author.

This research was supported by the National Engineering and Science Research Council of Canada and by the National Natural Science Foundation of China under grants 11271232 and 11201265.

[8] proposed a splitting wavelet method for solving the spatial aerosol dynamic equations on time, particle size and vertical coordinates. Due to the condensation advection and the nonlinear coagulation, modelling accurately and efficiently the sharp distributions of aerosols still is a challenge work in computation of the multi-component aerosol dynamic equations.

The multi-component aerosol dynamic equations are described as follows. Let $q_i(m, t)$ be the mass concentration distribution for species i of aerosol particles having total particle mass in the range m to $m + dm$ at time t . N_c is the total number of chemical species. The change rate of the total mass of a particle of mass m caused by condensation/evaporation is denoted by

$$(1) \quad I(m, t) = \sum_{i=1}^{N_c} I_i(m, t),$$

where $I_i = \frac{dm_i}{dt}$, m_i is the mass of species i in a particle of total mass m . The normalized condensation/evaporation rate of species i is

$$(2) \quad H_i(m, t) = \frac{1}{m} \frac{dm_i}{dt},$$

and the total condensation/evaporation rate is

$$(3) \quad H(m, t) = \sum_{i=1}^{N_c} \frac{1}{m} \frac{dm_i}{dt} = \sum_{i=1}^{N_c} H_i(m, t).$$

The multi-component aerosol general dynamic equations are ([11, 14, 15])

$$(4) \quad \begin{aligned} \frac{\partial q_i(m, t)}{\partial t} &= H_i(m, t) \sum_{j=1}^{N_c} q_j(m, t) - \frac{\partial(mq_i H)}{\partial m} \\ &+ \int_{M_{\min}}^{m-M_{\min}} \beta(m, m-m') q_i(m, t) \frac{\sum_{j=1}^{N_c} q_j(m-m', t)}{m-m'} dm' \\ &- q_i(m, t) \int_{M_{\min}}^{M_{\max}} \beta(m, m') \frac{\sum_{j=1}^{N_c} q_j(m', t)}{m'} dm', \quad t \in (0, T], m \in \Omega, \end{aligned}$$

$$(5) \quad q_i(M_{\min}, t) = 0, \quad t \in [0, T],$$

$$(6) \quad q_i(m, 0) = q_i^0(m), \quad m \in \Omega, \quad i = 1, 2, \dots, N_c,$$

where $t > 0$ is the time, and $T > 0$ is the time period; the finite mass interval $\Omega = [M_{\min}, M_{\max}]$ where $M_{\min} > 0$ is the minimal mass and $M_{\max} > 0$ is a finite maximal mass. $\beta(m, m')$ is the coagulation kernel function. Eq. (4) forms a system of N_c nonlinear integral-differential equations on time and particle mass.

In this paper, we develop and analyze a time second-order characteristic finite element method (FEM) for solving the multi-component aerosol dynamic equations by taking the advantage of characteristic technique, which can solve the problems accurately and efficiently. In our method, we first transfer the time derivative term and the advection-condensation term into the global derivative term along the characteristics and then approximate it by the difference operator along the characteristic curve, where more accurate solution can be obtained. For treating the nonlinear coagulation term, by using two previous time level values, we propose to use a time second-order extrapolation, i.e. a combination of previous two level values of coagulation terms along the characteristics. The developed characteristic FEM scheme is of second-order accuracy in time and can provide efficiently high accuracy solutions when using large time step sizes. The study of the method has been examined for

the aerosol dynamics equations (single component) that describes aerosol number distribution on time and particle volume [9]. In this paper, we will further extend the characteristic FEM scheme to solving the multi-component aerosol general dynamic equations governing multi-component aerosol mass distributions on time and particle mass. We analyze theoretically the developed characteristic FEM scheme to the nonlinear multicomponent aerosol dynamic systems based on the theory of variation method and the technique of prior estimate. We prove the error estimate of second order in time for the scheme. Numerical experiments are carried out for two-component and three-component aerosol dynamic problems with one modal and tri-modal log-normal initial distributions. Numerical results show that our method is of second order accuracy in time. The scheme improves the accuracy of the classic characteristic finite element method which is of first order in time. The dynamic behaviours of multi-component aerosol distributions are also simulated by the scheme for the multi-component aerosol problems of aerosol water, black carbon and sulfate components with different tri-modal log-normal initial distributions.

The paper is structured as follows. The second-order characteristic FEM for nonlinear multi-component aerosol dynamic equations is proposed in Section 2. The theoretical analysis of error estimate is done in Section 3. Numerical experiments are given in Section 4 and conclusion is addressed in Section 5.

2. The time second order characteristic FEM scheme

Consider the linear change rate of the mass due to the condensation/evaporatoin process [6]

$$(7) \quad I_i = \alpha_i m, \quad i = 1, 2, \dots, N_c; \quad I = \sum_{i=1}^{N_c} I_i.$$

Letting $\alpha = \sum_{i=1}^{N_c} \alpha_i$, we have that

$$(8) \quad H_i = \alpha_i, \quad i = 1, 2, \dots, N_c; \quad H = \sum_{i=1}^{N_c} H_i = \alpha.$$

The multi-component aerosol dynamic equations become

$$(9) \quad \begin{aligned} \frac{\partial q_i(m, t)}{\partial t} &= H_i \sum_{j=1}^{N_c} q_j(m, t) - H q_i(m, t) - H m \frac{\partial (q_i(m, t))}{\partial m} \\ &+ \int_{M_{\min}}^{m-M_{\min}} \beta(m', m-m') q_i(m', t) \frac{\sum_{j=1}^{N_c} q_j(m-m', t)}{m-m'} dm' \\ &- q_i(m, t) \int_{M_{\min}}^{M_{\max}} \beta(m, m') \frac{\sum_{j=1}^{N_c} q_j(m', t)}{m'} dm', \end{aligned}$$

$$(10) \quad q_i(M_{\min}, t) = 0, \quad t \in [0, T],$$

$$(11) \quad q_i(m, 0) = q_i^0(m), \quad m \in [M_{\min}, M_{\max}], \quad i = 1, 2, \dots, N_c.$$

Let the following notation for the nonlinear coagulation terms,

$$\begin{aligned}
(12) \quad \Phi_i(m, t, q_i(m, t), \sum_{j=1}^{N_c} q_j(m, t)) \\
= \int_{M_{\min}}^{m-M_{\min}} \beta(m', m-m') q_i(m', t) \frac{\sum_{j=1}^{N_c} q_j(m-m', t)}{m-m'} dm' \\
- q_i(m, t) \int_{M_{\min}}^{M_{\max}} \beta(m, m') \frac{\sum_{j=1}^{N_c} q_j(m', t)}{m'} dm'.
\end{aligned}$$

The equations (9) can be written in a short form as

$$\begin{aligned}
(13) \quad \frac{\partial q_i(m, t)}{\partial t} + Hm \frac{\partial(q_i(m, t))}{\partial m} + Hq_i(m, t) - H_i \sum_{j=1}^{N_c} q_j(m, t) \\
= \Phi_i(m, t, q_i(m, t), \sum_{j=1}^{N_c} q_j(m, t)),
\end{aligned}$$

$$(14) \quad q_i(M_{\min}, t) = 0, \quad t \in [0, T],$$

$$(15) \quad q_i(m, 0) = q_i^0(m), \quad m \in [M_{\min}, M_{\max}], \quad i = 1, 2, \dots, N_c.$$

Take time step $\Delta t = T/K$, where $K > 0$ is a positive integer, and the time level $t^k = k\Delta t$, $k = 1, 2, \dots, K$. Let Ω_h be the quasi-uniform mesh of the mass interval $\Omega = [M_{\min}, M_{\max}]$ with steps $\{h_i\}$, $i = 1, 2, \dots, N_h$ and let $h = \max\{h_i\}$. We denote the usual space of square integrated functions on Ω by $L^2(\Omega)$ with inner product (\cdot, \cdot) and norm $\|\cdot\|$. Let $H^s(\Omega)$ be the corresponding standard Sobolev space with norm $\|\cdot\|_s$, and define the space $H_0^1(\Omega) = \{\psi \in H^1(\Omega) : \psi(M_{\min}) = 0\}$. Define a standard finite element space by $W_h \subset H_0^1(\Omega)$ with index $l > 0$ and associated with Ω_h .

In the following, we will construct the time second-order characteristic scheme for approximating the solutions of the multi-component aerosol dynamic equations at time t^{k+1} . The characteristic curve X starting any mass point m at time $t = t^{k+1}$ is defined by:

$$(16) \quad \frac{dX(\tau; t^{k+1}, m)}{d\tau} = HX(\tau; t^{k+1}, m),$$

$$(17) \quad X(t^{k+1}; t^{k+1}, m) = m,$$

where τ is the characteristic direction associated with the differential operator

$$\frac{\partial q_i}{\partial t} + Hm \frac{\partial q_i}{\partial m}.$$

The global derivative operator along the characteristics is given as

$$(18) \quad \phi(m) \frac{\partial}{\partial \tau} = \frac{\partial}{\partial t} + Hm \frac{\partial}{\partial m},$$

where

$$(19) \quad \phi(m) = \left[\frac{m^2(1 - e^{-H\Delta t})}{\Delta t^2} + 1 \right]^{\frac{1}{2}}.$$

Then we get the weak form of (13): find $q_i : [0, T] \rightarrow H_0^1(\Omega)$, such that

$$(20) \quad \begin{aligned} & \left(\phi(m) \frac{\partial q_i}{\partial \tau}, \psi \right) + (Hq_i, \psi) - \left(H_i \sum_{j=1}^{N_c} q_j, \psi \right) \\ & = (\Phi_i(m, t, q_i(m, t), \sum_{j=1}^{N_c} q_j(m, t)), \psi), \quad \forall \psi \in H_0^1(\Omega). \end{aligned}$$

Let \bar{m} and $\bar{\bar{m}}$ be the intersection points of the characteristic curve (16) (17) at time level $t = t^k$ and $t = t^{k+1}$, respectively,

$$(21) \quad \bar{m} = me^{-H\Delta t}, \quad \bar{\bar{m}} = me^{-2H\Delta t}.$$

Then $\phi(m) \frac{\partial q_i}{\partial \tau}$ can be approximated by the characteristic difference operator as :

$$(22) \quad \phi(m) \frac{\partial q_i}{\partial \tau} \approx \phi(m) \frac{q_i(m, t^{k+1}) - q_i(\bar{m}, t^k)}{[(m - \bar{m})^2 + (\Delta t)^2]^{\frac{1}{2}}} = \frac{q_i(m, t^{k+1}) - q_i(\bar{m}, t^k)}{\Delta t}.$$

Further, by the technique of the time second-order extrapolation along the characteristics, we approximate the nonlinear coagulation terms by

$$(23) \quad \begin{aligned} & \Phi_i(m, t^{k+\frac{1}{2}}, q_i(m, t^{k+\frac{1}{2}}), \sum_{j=1}^{N_c} q_j(m, t^{k+\frac{1}{2}})) \\ & \approx \frac{3}{2} \Phi_i(\bar{m}, t^k, q_i^k(\bar{m}), \sum_{j=1}^{N_c} q_j^k(\bar{m})) - \frac{1}{2} \Phi_i(\bar{\bar{m}}, t^{k-1}, q_i^{k-1}(\bar{\bar{m}}), \sum_{j=1}^{N_c} q_j^{k-1}(\bar{\bar{m}})). \end{aligned}$$

The time second-order characteristic finite element scheme for (13) is proposed as: find $q_{i,h} \in W_h$, such that

$$(24) \quad \begin{aligned} & \left(\frac{q_{i,h}^{k+1}(m) - q_{i,h}^k(\bar{m})}{\Delta t}, \psi_h \right) + \left(H \frac{q_{i,h}^{k+1}(m) + q_{i,h}^k(\bar{m})}{2}, \psi_h \right) \\ & - \left(H_i \sum_{j=1}^{N_c} \frac{q_{j,h}^{k+1}(m) + q_{j,h}^k(\bar{m})}{2}, \psi_h \right) \\ & = \left(\frac{3}{2} \Phi_i(\bar{m}, q_{i,h}(\bar{m}, t^k), \sum_{j=1}^{N_c} q_{j,h}(\bar{m}, t^k)) - \frac{1}{2} \Phi_i(\bar{\bar{m}}, q_i(\bar{\bar{m}}, t^{k-1}), \sum_{j=1}^{N_c} q_{j,h}(\bar{\bar{m}}, t^{k-1})), \psi_h \right), \\ & \psi_h \in W_h, \quad i = 1, 2, \dots, N_c, \end{aligned}$$

subject to the initial values $q_{i,h}(m, 0) = Q_h q_i^0$, where the operator Q_h is the approximation project operator to W_h .

Since a combination of previous two level values of the coagulation terms is used, the derived scheme (24) is a linearized scheme. It is clear that the system (24) has the existence and uniqueness of the solution.

3. Error estimate

For a non-negative integer s , we define a function space Z^s by

$$(25) \quad Z^s = \{f \in C^j((0, t]; H^{s-j}(\Omega)), j = 0, 1, \dots, s, \|f\|_s < +\infty\}$$

where

$$(26) \quad \|f\|_s = \max\{\|f\|_{C^j((0, T]; H^{s-j}(\Omega))}, 0 \leq j \leq s\}.$$

From the standard interpolating theory [2], we have the following lemma.

Lemma 3.1. *For the finite element space W_h with index $l > 0$, there exists an interpolation operator $\pi_h : L_\infty(\Omega) \rightarrow W_h$ satisfying*

$$\|\psi - \pi_h \psi\|_r \leq Ch^{l+1-r} \|\psi\|_{l+1}, \quad \forall \psi \in H_0^1(\Omega) \cap H^{l+1}(\Omega), \quad r = 0, 1$$

with a positive constant C independent of h .

Theorem 3.1. *Let $\{q_{i,h}\}$ be the solution of the numerical scheme (24) over W_h with index $l > 0$ and according to the initial values $q_{i,h}^0 = \pi_h q_i^0$. Let $\{q_i\}$ be the solution of (13) which satisfies $q_i \in C^0(H^{l+1}) \cap H^1(H^l) \cap Z^3$, $1 \leq i \leq N_c$. Then there exists a positive constant $M > 0$ independent of h and Δt such that*

$$\max_{0 \leq k \leq K} \left(\sum_{i=1}^{N_c} \|q_i^k - q_{i,h}^k\|_0^2 \right)^{\frac{1}{2}} \leq M ((\Delta t)^2 + h^l).$$

Proof. Let $e_{i,h} = q_{i,h} - \pi_h q_i$, $e_h = \sum_{i=1}^{N_c} e_{i,h}$, and $\eta_i = q_i - \pi_h q_i$, $q = \sum_{i=1}^{N_c} q_i$, $\eta = \sum_{i=1}^{N_c} \eta_i$. Using these notations, from (13) and (24), we have the error equations as follows:

$$\begin{aligned} (27) \quad & \left(\frac{e_{i,h}^{k+1}(m) - e_{i,h}^k(\bar{m})}{\Delta t}, \psi \right) + \left(H \frac{e_{i,h}^{k+1}(m)}{2}, \psi \right) \\ & = - \left(H \frac{e_{i,h}^k(\bar{m})}{2}, \psi \right) + \left(H_i \frac{e_h^{k+1}(m)}{2}, \psi \right) + \left(H_i \frac{e_h^k(\bar{m})}{2}, \psi \right) \\ & \quad - \left(\frac{q_i^{k+1}(m) - q_i^k(\bar{m})}{\Delta t} - \left(\frac{\partial q_i}{\partial t} + Hm \frac{\partial q_i}{\partial m} \right) (t^{k+\frac{1}{2}}, m^*), \psi \right) \\ & \quad - \left(H \frac{q_i^{k+1}(m) + q_i^k(\bar{m})}{2} - H q_i^{k+\frac{1}{2}}(m^*), \psi \right) \\ & \quad + \left(H_i \frac{q^{k+1}(m) + q^k(\bar{m})}{2} - H_i q^{k+\frac{1}{2}}(m^*), \psi \right) + \left(\frac{\eta_i^{k+1}(m) - \eta_i^k(\bar{m})}{\Delta t}, \psi \right) \\ & \quad + \left(H \frac{\eta_i^{k+1}(m) + \eta_i^k(\bar{m})}{2}, \psi \right) - \left(H_i \frac{\eta^{k+1}(m) + \eta^k(\bar{m})}{2}, \psi \right) \\ & \quad + \left(\frac{3}{2} \Phi_i^k(\bar{m}, q_{i,h}^k(\bar{m}), q_h^k(\bar{m})) - \frac{1}{2} \Phi_i^{k-1}(\bar{m}, q_{i,h}^{k-1}(\bar{m}), q_h^{k-1}(\bar{m})) \right. \\ & \quad \left. - \Phi_i^{k+\frac{1}{2}}(m^*, q_i^{k+\frac{1}{2}}(m^*), q^{k+\frac{1}{2}}(m^*)), \psi \right) \\ & = I_1 + I_2 + I_3 + I_4 + I_5 + I_6 + I_7 + I_8 + I_9 + I_{10}, \end{aligned}$$

where $(t^{k+\frac{1}{2}}, m^*)$ is the middle point between (t^{k+1}, m) and (t^k, \bar{m}) along the characteristic curve, $m^* = \frac{m+\bar{m}}{2}$.

Choose $\psi = e_{i,h}^{k+1}$ in (27), and the zero extension is used that $q_i^k(\bar{m}) = 0$ and $\pi_h q_i^k(\bar{m}) = 0$ when $\bar{m} \leq M_{\min}$, $1 \leq i \leq N_c$. Firstly, noting that

$$\begin{aligned} \|e_{i,h}^k(\bar{m})\|_0^2 &= \int_{M_{\min}}^{M_{\max}} (e_{i,h}^k(m) e^{-H\Delta t})^2 dm \\ &\leq (1 + C_1 \Delta t) \int_{M_{\min}}^{M_{\max}} (e_{i,h}^k(y))^2 dy \leq (1 + C_1 \Delta t) \|e_{i,h}^k\|_0^2, \end{aligned}$$

we have that

$$(28) \quad I_1 \leq (1 + C_1 \Delta t) \|e_{i,h}^k\|_0^2 + C \|e_{i,h}^{k+1}\|_0^2.$$

Similarly, we have the estimations of I_2 and I_3

$$(29) \quad I_2 = \left(H_i \frac{e_h^{k+1}(m)}{2}, e_{i,h}^{k+1}(m) \right) = \left(H_i \frac{\sum_{j=1}^{N_C} e_{j,h}^{k+1}(m)}{2}, e_{i,h}^{k+1}(m) \right) \\ \leq C \sum_{j=1}^{N_C} \|e_{j,h}^{k+1}\|_0^2 + C \|e_{i,h}^{k+1}\|_0^2,$$

$$(30) \quad I_3 \leq (1 + C_1 \Delta t) \sum_{j=1}^{N_C} \|e_{j,h}^k\|_0^2 + C \|e_{i,h}^{k+1}\|_0^2.$$

For the term of I_4 , let $\Delta l = ((\Delta t)^2 + (m - me^{-H\Delta t})^2)^{\frac{1}{2}}$, and by using Taylor's expansion along the characteristic line at the point $(t^{k+\frac{1}{2}}, m^*)$, we have that

$$(31) \quad q_i^{k+1}(m) = q_i^{k+\frac{1}{2}}(m^*) + \frac{\Delta l}{2} \left(\frac{\partial q_i}{\partial \tau} \right)^{k+\frac{1}{2}}(m^*) \\ + \frac{(\frac{\Delta l}{2})^2}{2!} \left(\frac{\partial^2 q_i}{\partial \tau^2} \right)^{k+\frac{1}{2}}(m^*) + \frac{(\frac{\Delta l}{2})^3}{3!} \left(\frac{\partial^3 q_i}{\partial \tau^3} \right)(t', m'),$$

$$(32) \quad q_i^k(\bar{m}) = q_i^{k+\frac{1}{2}}(m^*) - \frac{\Delta l}{2} \left(\frac{\partial q_i}{\partial \tau} \right)^{k+\frac{1}{2}}(m^*) \\ + \frac{(\frac{\Delta l}{2})^2}{2!} \left(\frac{\partial^2 q_i}{\partial \tau^2} \right)^{k+\frac{1}{2}}(m^*) - \frac{(\frac{\Delta l}{2})^3}{3!} \left(\frac{\partial^3 q_i}{\partial \tau^3} \right)(t'', m''),$$

which leads to

$$(33) \quad q_i^{k+1}(m) - q_i^k(\bar{m}) = \Delta l \left(\frac{\partial q_i}{\partial \tau} \right)^{k+\frac{1}{2}}(m^*) + C((\Delta t)^3).$$

Thus

$$(34) \quad I_4 \leq C(\Delta t)^4 + C \|e_{i,h}^{k+1}\|_0^2.$$

By the following Taylor's expansion of $q_i^{k+1}(m)$ and $q_i^k(\bar{m})$ at the point $(t^{k+\frac{1}{2}}, m^*)$

$$(35) \quad q_i^{k+1}(m) = q_i^{k+\frac{1}{2}}(m^*) + (m - m^*) \left(\frac{\partial q_i}{\partial m} \right)^{k+\frac{1}{2}}(m^*) \\ + \frac{\Delta t}{2} \left(\frac{\partial q_i}{\partial t} \right)^{k+\frac{1}{2}}(m^*) + \left(\frac{1}{4}(\Delta t)^2 + (m - m^*)^2 \right) \frac{\partial^2 q_i}{\partial \tau^2}(t', m'),$$

$$(36) \quad q_i^k(\bar{m}) = q_i^{k+\frac{1}{2}}(m^*) + (\bar{m} - m^*) \left(\frac{\partial q_i}{\partial m} \right)^{k+\frac{1}{2}}(m^*) \\ - \frac{\Delta t}{2} \left(\frac{\partial q_i}{\partial t} \right)^{k+\frac{1}{2}}(m^*) + \left(\frac{1}{4}(\Delta t)^2 + (\bar{m} - m^*)^2 \right) \frac{\partial^2 q_i}{\partial \tau^2}(t', m'),$$

we obtain

$$(37) \quad I_5 \leq C(\Delta t)^4 + \|e_{i,h}^{k+1}\|_0^2.$$

Similarly, we can get the estimate of the I_6 ,

$$\begin{aligned}
(38) \quad I_6 &= \left(H_i \frac{q^{k+1}(m) + q^k(\bar{m})}{2} - H_i q^{k+\frac{1}{2}}(m^*), e_{i,h}^{k+1} \right) \\
&= \left(H_i \sum_{j=1}^{N_c} \left(\frac{q_j^{k+1}(m) + q_j^k(\bar{m})}{2} - q_j^{k+\frac{1}{2}}(m^*) \right), e_{i,h}^{k+1} \right) \\
&\leq C(\Delta t)^4 + C\|e_{i,h}^{k+1}\|_0^2.
\end{aligned}$$

For the term of I_7 , it holds that

$$\begin{aligned}
(39) \quad I_7 &= \left(\frac{\eta_i^{k+1}(m) - \eta_i^k(\bar{m})}{\Delta t}, e_{i,h}^{k+1} \right) \\
&= \left(\frac{(\eta_i^{k+1}(m) - \eta_i^k(m)) + (\eta_i^k(m) - \eta_i^k(\bar{m}))}{\Delta t}, e_{i,h}^{k+1} \right) \\
&= \left(\frac{\eta_i^{k+1}(m) - \eta_i^k(m)}{\Delta t}, e_{i,h}^{k+1} \right) + \left(\frac{\eta_i^k(m) - \eta_i^k(\bar{m})}{\Delta t}, e_{i,h}^{k+1} \right) = I_{7,1} + I_{7,2}.
\end{aligned}$$

We have that

$$\begin{aligned}
I_{7,1} &= \left(\frac{\eta_i^{k+1}(m) - \eta_i^k(m)}{\Delta t}, e_{i,h}^{k+1} \right) = \frac{1}{\Delta t} \int_{\Omega} \left[\int_{t^k}^{t^{k+1}} \frac{\partial \eta_i}{\partial t} dt \right] e_{i,h}^{k+1} dm \\
&\leq C\|e_{i,h}^{k+1}\|_0^2 + C \frac{1}{\Delta t} \left\| \frac{\partial \eta}{\partial t} \right\|_{L^2(t^k, t^{k+1}; L^2)}^2,
\end{aligned}$$

and

$$I_{7,2} = \left(\frac{\eta_i^k(m) - \eta_i^k(\bar{m})}{\Delta t}, e_{i,h}^{k+1} \right) \leq Ch^{2l} + C\|e_{i,h}^{k+1}\|_0^2,$$

and thus

$$(40) \quad I_7 \leq Ch^{2l} + C\|e_{i,h}^{k+1}\|_0^2 + C \frac{1}{\Delta t} \left\| \frac{\partial \eta}{\partial t} \right\|_{L^2(t^k, t^{k+1}; L^2)}^2.$$

Similarly as (28), we have the estimations of I_8 and I_9

$$(41) \quad I_8 = \left(H \frac{\eta_i^{k+1}(m) + \eta_i^k(\bar{m})}{2}, e_{i,h}^{k+1}(m) \right) \leq C(h^{2l+2} + \|e_{i,h}^{k+1}\|_0^2).$$

$$\begin{aligned}
(42) \quad I_9 &= - \left(H_i \frac{\sum_{j=1}^{N_c} (\eta_j^{k+1}(m) + \eta_j^k(\bar{m}))}{2}, e_{i,h}^{k+1} \right) \\
&\leq C(h^{2l+2} + \|e_{i,h}^{k+1}\|_0^2).
\end{aligned}$$

For the coagulation term of I_{10} , we have that

$$\begin{aligned}
(43) \quad I_{10} &= \left(\frac{3}{2} \Phi_i^k(\bar{m}, q_{i,h}^k(\bar{m}), q_h^k(\bar{m})) - \frac{1}{2} \Phi_i^{k-1}(\bar{m}, q_{i,h}^{k-1}(\bar{m}), q_h^{k-1}(\bar{m})) \right. \\
&\quad \left. - \Phi_i^{k+\frac{1}{2}}(m^*, q_i^{k+\frac{1}{2}}(m^*), q^{k+\frac{1}{2}}(m^*)), e_{i,h}^{k+1} \right) \\
&= \left(\frac{3}{2} \Phi_i^k(\bar{m}, q_{i,h}^k(\bar{m}), q_h^k(\bar{m})) - \frac{3}{2} \Phi_i^k(\bar{m}, q_i^k(\bar{m}), q^k(\bar{m})), e_{i,h}^{k+1} \right) \\
&\quad + \left(\frac{1}{2} \Phi_i^{k-1}(\bar{m}, q_i^{k-1}(\bar{m}), q^{k-1}(\bar{m})) \right. \\
&\quad \left. - \frac{1}{2} \Phi_i^{k-1}(\bar{m}, q_{i,h}^{k-1}(\bar{m}), q_h^{k-1}(\bar{m})), e_{i,h}^{k+1} \right) \\
&\quad + \left(\frac{3}{2} \Phi_i^k(\bar{m}, q_i^k(\bar{m}), q^k(\bar{m})) - \frac{1}{2} \Phi_i^{k-1}(\bar{m}, q_i^{k-1}(\bar{m}), q^{k-1}(\bar{m})) \right. \\
&\quad \left. - \Phi_i^{k+\frac{1}{2}}(m^*, q_i^{k+\frac{1}{2}}(m^*), q^{k+\frac{1}{2}}(m^*)), e_{i,h}^{k+1} \right) \\
&= I_{10,1} + I_{10,2} + I_{10,3}.
\end{aligned}$$

We make an induction hypothesis that there exists a positive constant $C^* > 0$ such that

$$(44) \quad \sup_{0 \leq k \leq K} \|q_{i,h}^k\|_0 \leq C^*, \quad 1 \leq i \leq N_c,$$

which will be proved later.

We start from considering the first part of Φ_i in $I_{10,1}$

$$\begin{aligned}
(45) \quad &\left(\int_{M_{\min}}^{\bar{m}-M_{\min}} \beta(m', \bar{m} - m') q_{i,h}^k(m') \frac{q_h^k(\bar{m} - m')}{\bar{m} - m'} dm' \right. \\
&\quad \left. - \int_{M_{\min}}^{\bar{m}-M_{\min}} \beta(m', \bar{m} - m') q_i^k(m') \frac{q^k(\bar{m} - m')}{\bar{m} - m'} dm', e_{i,h}^{k+1} \right) \\
&= \int_{\Omega} \left[\int_{M_{\min}}^{\bar{m}-M_{\min}} \beta(m', \bar{m} - m') (q_{i,h}^k(m') - q_i^k(\bar{m})) \right. \\
&\quad \left. \frac{q_h^k(\bar{m} - m')}{\bar{m} - m'} dm' \right] e_{i,h}^{k+1} dm \\
&\quad + \int_{\Omega} \left[\int_{M_{\min}}^{\bar{m}-M_{\min}} \beta(m', \bar{m} - m') q_i^k(m') \right. \\
&\quad \left. \frac{(q_h^k(\bar{m} - m') - q^k(\bar{m} - m'))}{\bar{m} - m'} dm' \right] e_{i,h}^{k+1} dm \\
&= L_{1,1} + L_{1,2}.
\end{aligned}$$

Noting that the positive coagulation term equals zero whenever the upper integration limit is smaller than the smaller limit in [13]. Let $\Omega' = \{m \in \Omega; 2M_{\min} \leq \bar{m} \leq$

M_{max} }, and using the Holder inequality, we obtain that

$$(46) \quad L_{1,1} \leq C\beta_{\max} \int_{\Omega'} \left(\int_{M_{\min}}^{\bar{m}-M_{\min}} (q_{i,h}^k(m') - q_i^k(m'))^2 dm' \right)^{\frac{1}{2}} \\ \left(\int_{M_{\min}}^{\bar{m}-M_{\min}} (q_h^k(\bar{m} - m')^2 dm' \right)^{\frac{1}{2}} e_{i,h}^{k+1} dm,$$

$$(47) \quad L_{1,2} \leq C\beta_{\max} \int_{\Omega'} \left(\int_{M_{\min}}^{\bar{m}-M_{\min}} (q_i^k(m'))^2 dm' \right)^{\frac{1}{2}} \\ \left(\int_{M_{\min}}^{\bar{m}-M_{\min}} \left(\sum_{j=1}^{N_c} (q_{j,h}^k(\bar{m} - m') - q_j^k(\bar{m} - m')) \right)^2 dm' \right)^{\frac{1}{2}} e_{i,h}^{k+1} dm,$$

where $M_{\min} \leq \bar{m} - m \leq M_{max} - M_{\min}$. Letting $z = \bar{m} - m'$, noting that $q_i(z) = 0$ and $q_{i,h}(z) = 0$, $1 \leq i \leq N_c$, when $z \leq M_{\min}$, then it holds

$$(48) \quad \int_{M_{\min}}^{\bar{m}-M_{\min}} (q_{i,h}^k(\bar{m} - m) - q_i^k(\bar{m} - m))^2 dm \\ \leq \int_{\Omega} (q_{i,h}^k(z) - q_i^k(z))^2 dz,$$

and by the induction hypothesis (44), we have that

$$(49) \quad L_{1,1} \leq C(\|e_{i,h}^k(\bar{m})\|_0 + \|\eta_i^k(\bar{m})\|_0) \|e_{i,h}^{k+1}\|_0, \\ L_{1,2} \leq C \left(\sum_{j=1}^{N_c} (\|e_{j,h}^k(\bar{m})\|_0 + \|\eta_j^k(\bar{m})\|_0) \right) \|e_{i,h}^{k+1}\|_0.$$

Further, estimating the second part of Φ_i in $I_{10,1}$, we get that

$$(50) \quad \left(\int_{M_{\min}}^{M_{\max}} q_{i,h}^k(\bar{m}) \beta(\bar{m}, m') \frac{q_h^k(m')}{m'} dm' \right. \\ \left. - \int_{M_{\min}}^{M_{\max}} q_i^k(\bar{m}) \beta(\bar{m}, m') \frac{q^k(m')}{m'} dm', e_{i,h}^{k+1} \right) \\ = \int_{\Omega} \left(\int_{M_{\min}}^{M_{\max}} q_{i,h}^k(\bar{m}) \beta(\bar{m}, m') \frac{\sum_{j=1}^{N_c} (q_{j,h}^k(m') - q_j^k(m'))}{m'} dm' \right. \\ \left. + \int_{M_{\min}}^{M_{\max}} (q_{i,h}^k(\bar{m}) - q_i^k(\bar{m})) \beta(\bar{m}, m') \frac{\sum_{j=1}^{N_c} q_j^k(m')}{m'} dm' \right) e_{i,h}^{k+1} dm \\ \leq C \left(\sum_{j=1}^{N_c} (\|e_{j,h}^k\|_0 + \|\eta_{j,h}^k\|_0) + \|e_{i,h}^k(\bar{m})\|_0 + \|\eta_i^k(\bar{m})\|_0 \right) \|e_{i,h}^{k+1}\|_0.$$

Thus, we have that

$$(51) \quad I_{10,1} \leq C \left(\sum_{j=1}^{N_c} (\|e_{j,h}^k\|_0 + \|\eta_j\|_0) + \|e_{i,h}^k(\bar{m})\|_0 + \|\eta^k(\bar{m})\|_0 \right) \|e_{i,h}^{k+1}\|_0 \\ \leq C(1 + C_1 \Delta t) \left(\sum_{j=1}^{N_c} (\|e_{j,h}^k\|_0 + \|\eta_j^k\|) \right) \|e_{i,h}^{k+1}\|_0.$$

Similarly, we have the estimate to $I_{10,2}$

$$(52) \quad I_{10,2} \leq C(1 + C_1 \Delta t) \left(\sum_{j=1}^{N_c} (\|e_{j,h}^{k-1}\|_0 + \|\eta_j^{k-1}\|) \right) \|e_{i,h}^{k+1}\|_0.$$

For the term of $I_{10,3}$, noting that

$$\left\| \frac{\partial^2}{\partial \tau^2} \Phi_i(m, q_i(m, t), q(m, t)) \right\|_{L^2((t^{k-1}, t^{k+1}], L^2)} \leq C \max_{t \in (t^{k-1}, t^{k+1}]} \sum_{j=1}^{N_c} \|q_j(m, t)\|_2,$$

and by Taylor's expansion to $\Phi_i(m, q_i(m, t), q(m, t))$ along the characteristic curve at the point $(m^*, t^{k+\frac{1}{2}})$, we can get

$$(53) \quad I_{10,3} = \left(\frac{3}{2} \Phi_i^k(\bar{m}, q_i^k(\bar{m}), q^k(\bar{m})) - \frac{1}{2} \Phi_i^{k-1}(\bar{m}, q_i^{k-1}(\bar{m}), q^{k-1}(\bar{m})) \right. \\ \left. - \Phi_i^{k+\frac{1}{2}}(m^*, q_i^{k+\frac{1}{2}}(m^*), q^{k+\frac{1}{2}}(m^*)), e_{i,h}^{k+1} \right) \\ \leq C \left((\Delta t)^4 \left\| \frac{\partial^2}{\partial \tau^2} \Phi_i(m, q_i(m, t), q(m, t)) \right\|_{L^2((t^{k-1}, t^{k+1}], L^2)} + \|e_{i,h}^{k+1}\|_0^2 \right) \\ \leq C((\Delta t)^4 + \|e_{i,h}^{k+1}\|_0^2).$$

Therefore, the estimation of I_{10} is obtained as

$$(54) \quad I_{10} \leq C(1 + \Delta t) \left(\sum_{j=1}^{N_c} \|e_{j,h}^k\|^2 + \sum_{j=1}^{N_c} \|e_{j,h}^{k-1}\|_0^2 + h^{2l+2} \right) + C \left((\Delta t)^4 + \|e_{i,h}^{k+1}\|_0^2 \right).$$

Noting that

$$(55) \quad \|e_{i,h}^k(\bar{m})\|_0^2 \leq (1 + C_1 \Delta t) \|e_{i,h}^k\|_0^2.$$

we have the estimate for the left-hand side term in (27)

$$(56) \quad \left(\frac{e_{i,h}^{k+1}(m) - e_{i,h}^k(\bar{m})}{\Delta t}, e_{i,h}^{k+1} \right) \\ \geq \frac{1}{2\Delta t} (\|e_{i,h}^{k+1}(m)\|_0^2 - \|e_{i,h}^k(\bar{m})\|_0^2 + \|e_{i,h}^{k+1}(m) - e_{i,h}^k(\bar{m})\|_0^2) \\ \geq \frac{1}{2\Delta t} (\|e_{i,h}^{k+1}\|_0^2 - \|e_{i,h}^k\|_0^2) - \frac{C_0}{2} \|e_{i,h}^k\|_0^2.$$

From the estimations of $I_1 - I_{10}$, and (56), we can get

$$\begin{aligned}
(57) \quad & \frac{1}{2\Delta t} (\|e_{i,h}^{k+1}\|_0^2 - \|e_{i,h}^k\|_0^2) + \frac{H}{2} \|e_{i,h}^{k+1}\|_0^2 \\
& \leq C \sum_{j=1}^{N_c} \|e_{j,h}^{k+1}\|_0^2 + C(1 + C_1\Delta t) \sum_{j=1}^{N_c} \|e_{j,h}^k\|_0^2 \\
& \quad + C(1 + C_1\Delta t) \sum_{j=1}^{N_c} \|e_{j,h}^{k-1}\|_0^2 + C(\Delta t)^4 + C(1 + C_1\Delta t)h^{2l+2} + Ch^{2l},
\end{aligned}$$

for $1 \leq i \leq N_c$. Multiplying the above equations by $2\Delta t$ and summing them from $i = 1$ to N_c , we can get that

$$\begin{aligned}
(58) \quad & \left(\sum_{i=1}^{N_c} \|e_{i,h}^{k+1}\|_0^2 - \sum_{i=1}^{N_c} \|e_{i,h}^k\|_0^2 \right) + \Delta t H \sum_{i=1}^{N_c} \|e_{i,h}^{k+1}\|_0^2 \\
& \leq 2\Delta t C \left\{ \sum_{i=1}^{N_c} \|e_{i,h}^{k+1}\|_0^2 + (1 + C_1\Delta t) \sum_{i=1}^{N_c} \|e_{i,h}^k\|_0^2 \right. \\
& \quad \left. + (1 + C_1\Delta t) \sum_{i=1}^{N_c} \|e_{i,h}^{k-1}\|_0^2 + (\Delta t)^4 + (1 + C_1\Delta t)h^{2l+2} + h^{2l} \right\}.
\end{aligned}$$

Thus, applying the Gronwall's lemma, we finally get that

$$(59) \quad \left(\sum_{i=1}^{N_c} \|e_{i,h}^n\|_0^2 \right)^{\frac{1}{2}} \leq C\{(\Delta t)^2 + h^l\}, \quad \forall n = 1, 2, \dots, K.$$

Now, we prove the induction hypothesis (44). First, we have that

$$\begin{aligned}
(60) \quad & \|q_{i,h}^0\|_0 = \|\pi_h q_i^0\|_0 \leq \|q_i^0 - \pi_h q_i^0\|_0 + \|q_i^0\|_0 \\
& \leq Ch^{l+1} \|q_i^0\|_{l+1} + \|q_i^0\|_0 \leq C^*.
\end{aligned}$$

If the induction hypothesis (44) is false, there exists an integer k^* such that

$$(61) \quad \|q_{i,h}^k\|_0 \leq C^*, \quad \text{for } 0 \leq k \leq k^* - 1; \quad \|q_{i,h}^{k^*}\|_0 > C^*.$$

From the result of (59), we can know that

$$(62) \quad \|\pi_h q_i^{k^*} - q_{i,h}^{k^*}\|_0 = \|e_{i,h}^{k^*}\|_0 \leq C\{(\Delta t)^2 + h^l\},$$

when h and Δt are small enough, we can conclude that

$$\begin{aligned}
(63) \quad & \|q_{i,h}^{k^*}\|_0 \leq \|q_i^{k^*} - \pi_h q_i^{k^*}\|_0 + \|\pi_h q_i^{k^*} - q_{i,h}^{k^*}\|_0 + \|q_i^{k^*}\|_0 \\
& \leq Ch^{l+1} + C\{(\Delta t)^2 + h^2\} + \|q_i^{k^*}\|_0 \leq C^*,
\end{aligned}$$

which is contradict to (61). This proves the induction hypothesis (44). The proof of the theorem completes.

4. Numerical experiments

In this section, we present numerical experiments of solving the multi-component aerosol dynamic equation by our time second-order characteristic FEM scheme. We first consider a condensation-evaporation problem of two-component aerosols, which examines the accuracy of our method. A more general condensation problem of three-component aerosols is then simulated, which shows the dynamic behaviour of the multi-component aerosols. Finally, the three-component aerosols of aerosol water, black carbon and sulfate are computed with a tri-modal log-normal initial

distribution and the different tri-modal log-normal initial distributions of three-component aerosols. The results show our method second order accuracy in time, which improves first order results of the classical characteristic FEM scheme.

Let $q_{i,h}(T)$ and $q_i^A(T)$ be the numerical solution and the analytical solution of i 'the component at time T in the numerical tests, respectively. The errors are measured in the relative discrete L_2 norm and the relative discrete L_∞ norm:

$$(64) \quad E_\infty = \frac{\max_{1 \leq i \leq N_c} \|q_{i,h}(T) - q_i^A(T)\|_\infty}{\max_{1 \leq i \leq N_c} \|q_i^A(T)\|_\infty}$$

$$(65) \quad E_2 = \frac{(\sum_{i=1}^{N_c} \|q_{i,h}(T) - q_i^A(T)\|_0^2)^{\frac{1}{2}}}{(\sum_{i=1}^{N_c} \|q_i^A(T)\|_0^2)^{\frac{1}{2}}}.$$

Example 1. Consider the multi-component aerosol dynamic equation (13) with the following initial distribution of q_i^0

$$(66) \quad q_i^0(m) = c \frac{m}{\hat{m}_c} \exp\left(-\gamma \left(\frac{m}{\hat{m}_c}\right)^2\right), \quad i = 1, 2,$$

where $\gamma = 0.1$, $\hat{m}_c = 3.2 \times 10^{-13}$ g is a characteristic value of m , and $c = 10$. Two different cases are performed, one with condensation only, and the other with evaporation/condensation, and both with $H_i(m, t) = \alpha_i$ constant.

The numerical results of the condensation only problem are shown in Fig. 1. Particle mass was converted to particle diameter for the purpose of plotting the distribution, the particle density $\rho = 1$ g cm⁻³. The normalized condensation rates for the two different species are $\alpha_1 = 7 \times 10^{-2}$ hour⁻¹ and $\alpha_2 = 5 \times 10^{-2}$ hour⁻¹, respectively. We can see from the figures that under the impact of the condensation process, there are increases in the mass of both species in the aerosol particles, which then cause the distributions of two species and total mass shift towards the bigger particle domain.

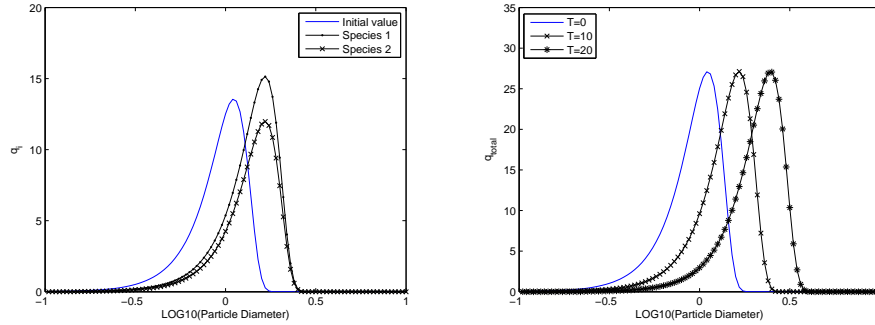


FIGURE 1. Numerical solutions of the mass distribution of species 1 and 2 at time $T = 10$ hours (left) and numerical solutions of the total mass distribution at time $T = 10$ h and $T = 20$ h (right) for the only condensation problem. $\alpha_1 = 7 \times 10^{-2}$ hour⁻¹, $\alpha_2 = 5 \times 10^{-2}$ hour⁻¹, $M_{\min} = 5.236 \times 10^{-16}$ g, $M_{\max} = 5.236 \times 10^{-10}$ g.

The errors and ratios in time step of the results at time $T = 5$ hours are shown in Table 1. As the problem has no exact solution available, we use the reference analytical solution obtained by fine mesh in calculation of errors E_∞ and E_2 norm.

From the table, it is clearly shown that our method has second-order accuracy in time.

TABLE 1. Errors and ratios in time step of our scheme for the two-component aerosol condensation problem.

Δt (hour)	$\frac{1}{15}$	$\frac{1}{16}$	$\frac{1}{17}$	$\frac{1}{18}$
E_∞	6.3910e-6	5.6082e-6	4.9137e-6	4.2933e-6
Ratio	-	2.0246	2.1809	2.3613
E_2	4.1161e-6	3.6141e-6	3.1682e-6	2.7696e-6
Ratio	-	2.0153	2.1718	2.3526

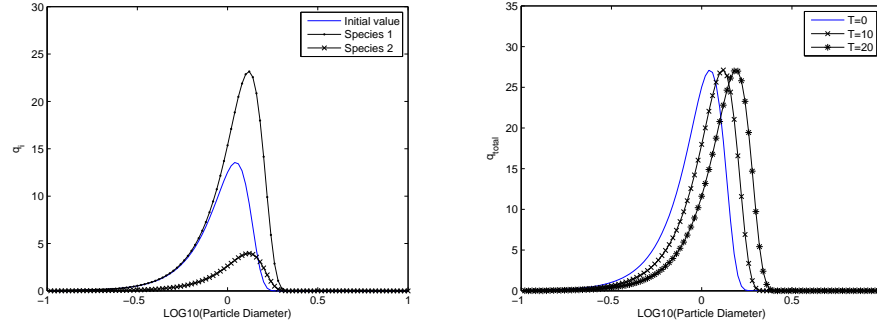


FIGURE 2. Numerical solutions of the mass distribution of species 1 and 2 at time $T = 10$ hour (left) and numerical solutions of the total mass distribution at time $T = 10$ hour and $T = 20$ hour (right) for the condensation and evaporation problem. $\alpha_1 = 7 \times 10^{-2} \text{ hour}^{-1}$, $\alpha_2 = -2 \times 10^{-2} \text{ hour}^{-1}$, $M_{\min} = 5.236 \times 10^{-16} \text{g}$, $M_{\max} = 5.236 \times 10^{-10} \text{g}$.

The second case considers a combination problem of the condensation of species 1 and the evaporation of species 2. The normalized condensation rate of species 1 is $\alpha_1 = 7 \times 10^{-2} \text{ hour}^{-1}$ while the evaporation rate of species 2 is $\alpha_2 = -2 \times 10^{-2} \text{ hour}^{-1}$. Numerical results are showed in Fig. 2 at time $T = 10$ hour. We can see that due to the evaporation of the species 2, though the position of the peak of the total mass still moves towards to a large size value, but much slower than the previous case in Fig. 1.

Example 2. Consider the multi-component aerosol system (13) including three components in the condensation process. The initial distribution of each species is as same as (66) and with same parameters except for $\hat{m}_c = 2.8 \times 10^{-13}$ in this example. The normalized condensation rates of the three species are $\alpha_1 = 9 \times 10^{-2} \text{ hour}^{-1}$, $\alpha_2 = 7 \times 10^{-9} \text{ hour}^{-1}$ and $\alpha_3 = 5 \times 10^{-9} \text{ hour}^{-1}$, respectively.

Fig. 3 shows the predicted mass distributions of species 1, 2 and 3 at time $T = 10$ hours and the numerical solutions of the total mass distribution at time $T = 10$ hours and $T = 20$ hours. As shown in the figure, with one more species included in the aerosol particles, the size distribution of the total mass shifts much faster undergoing the condensation process. Meanwhile, bigger condensation rate leads

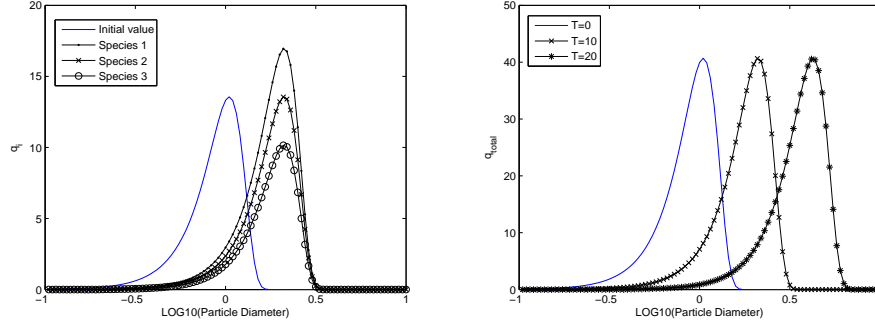


FIGURE 3. Numerical solutions of the mass distributions of species 1, 2 and 3 at time $T = 10$ (right) and numerical solutions of the total mass distribution at time $T = 10$ and $T = 20$ (left), for the condensation problem. $\alpha_1 = 9 \times 10^{-9}$ hour $^{-1}$, $\alpha_2 = 7 \times 10^{-9}$ hour $^{-1}$, $\alpha_3 = 5 \times 10^{-9}$ hour $^{-1}$, $M_{\min} = 5.236 \times 10^{-16}$ g, $M_{\max} = 5.236 \times 10^{-10}$ g.

to larger mass proportion as time increases.

Example 3. Now, consider the multi-component aerosol general dynamic problem with a tri-modal log-normal initial distribution for each species, where each modal represents the nucleation mode, accumulation mode and coarse mode, respectively. The initial distribution is given as

$$(67) \quad q_i^0(m) = \sum_{j=1}^3 \frac{M_{c,j}}{\sqrt{2\pi} \ln \sigma_{m,j}} \exp\left(-\frac{\ln^2(m/m_{g,j})}{\ln^2 \sigma_{m,j}}\right), i = 1, 2, 3,$$

where $\sigma_{m,j}$ is the geometric mass standard deviation, and $m_{g,j}$ is the geometric mean mass. The values of the parameters are listed in Table 2. The concerned domain is $\Omega = [5.236 \times 10^{-22}, 5.236 \times 10^{-7}]$.

TABLE 2. Tri-modal log-normal parameters.

	Nucleation mode	Accumulation mode	Coarse mode
$M_{c,j}$ (g)	7.22×10^1	1.2×10^2	8.22×10^1
$m_{g,j}$ (g)	1.15×10^{-18}	3.7×10^{-16}	4.8×10^{-13}
$\sigma_{m,j}$	1.7	2.03	2.15

Take the condensation rates of the three species $\alpha_1 = 9 \times 10^{-2}$ hour $^{-1}$, $\alpha_2 = 7 \times 10^{-9}$ hour $^{-1}$ and $\alpha_3 = 3 \times 10^{-9}$ hour $^{-1}$, respectively. Table 3 presents the comparison of the errors and ratios in time step of the predicted results by our method and the standard characteristics FEM scheme (S-C-FEM). The results in the table clearly show that for the complex multi-component aerosol dynamics problem with different multi-modal distributions, our method can obtain excellent solutions. Our method is of second-order accuracy in time step, while the S-C-FEM is only of first-order accuracy in time step. The mass distributions of three species and the numerical solutions of the total mass distribution are presented in Fig. 4. The geometric mean mass for all the three modes of the distributions of three species increase in the condensation process.

TABLE 3. Comparison of errors and ratios in time step at $T = 5$ hour for the three-component aerosol condensation problem with Tri-modal initial distribution by our method and the classical characteristic FEM scheme (S-C-FEM).

	Δt (hour)	$\frac{T}{4}$	$\frac{T}{8}$	$\frac{T}{16}$	$\frac{T}{32}$	$\frac{T}{48}$
Our method	E_∞	7.2623e-4	1.8012e-4	4.5590e-5	1.1647e-5	5.1129e-6
	Ratio	-	2.0115	1.9821	1.9688	2.0304
	E_2	6.6488e-4	1.6511e-4	4.0835e-5	1.0017e-5	4.3450e-6
	Ratio	-	2.0096	2.0155	2.0273	2.0601
S-C-FEM	E_∞	1.6111e-2	8.2048e-3	3.9650e-3	1.7671e-3	1.0225e-3
	Ratio	-	0.9735	1.0491	1.1659	1.3493
	E_2	1.4741e-2	7.5070e-3	3.6289e-3	1.6178e-3	9.3620e-4
	Ratio	-	0.9736	1.0487	1.1655	1.3490

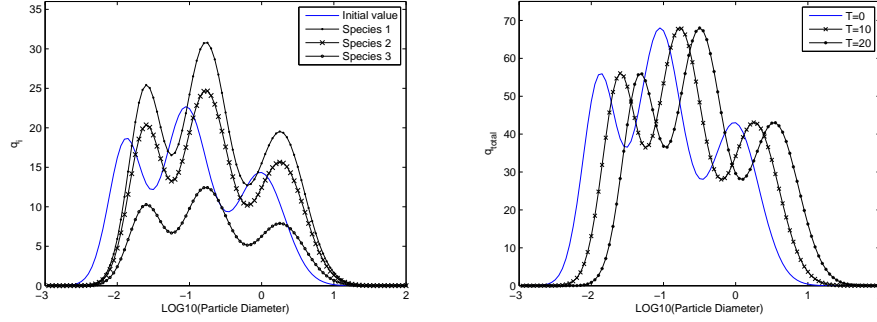


FIGURE 4. Numerical solutions of the mass distributions of species 1, 2 and 3 at time $T = 10$ (left) and numerical solutions of the total mass distribution at time $T = 5$ and $T = 20$ (right), for the condensation problem. $\alpha_1 = 9 \times 10^{-9}$ hour $^{-1}$, $\alpha_2 = 7 \times 10^{-9}$ hour $^{-1}$, $\alpha_3 = 3 \times 10^{-9}$ hour $^{-1}$, $M_{\min} = 5.236 \times 10^{-22}$ g, $M_{\max} = 5.236 \times 10^{-7}$ g.

Example 4. Finally, we simulate the multi-component aerosol general dynamic problem of aerosol water, black carbon and sulfate components with different tri-modal log-normal initial distributions. The three initial distributions are shown in Fig. 5 (left).

We solve the general problem on the $\Omega = [5.236 \times 10^{-22}, 5.236 \times 10^{-7}]$ g and time interval $[0, T] = [0, 5]$ hours. The predicted mass concentration distributions of the of aerosol water, black carbon and sulfate components are shown in Fig. 5. The initial concentration distribution and the numerical result of the aerosol total mass are given in Fig. 6. We can see that the peaks of the distributions of aerosol water, black carbon and sulfate components change a lot during the simulation. For example, at time $T = 0$, the mass distribution of aerosol water has the highest peak value of 31.74 in the coarse mode, while at time $T = 5$, the highest peak value is 176.12 located in the accumulation mode. Due to the highest condensation rate among the three species, the concentration of aerosol water is the smallest at time $T = 0$ hour, but becomes the largest at time $T = 5$ hours. For the distribution

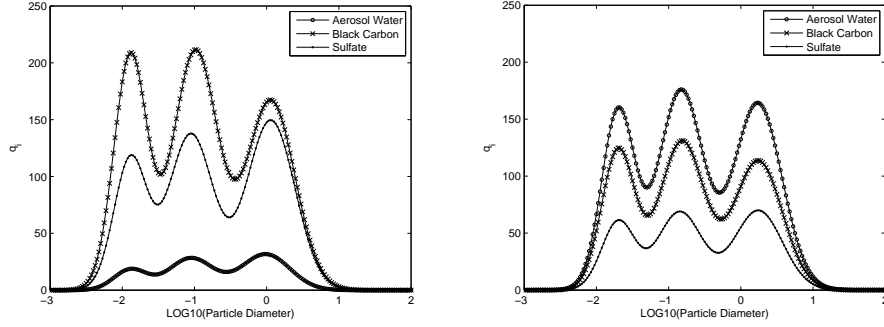


FIGURE 5. Initial distributions of the mass concentrations of aerosol water, black carbon and sulfate components (left) and the numerical solutions at time $T = 5$ hours (right) for the multi-component condensation problem. The condensation rates of the aerosol water (aw), black carbon (bc) and sulfate (sul) are $\alpha_{aw} = 1.6 \times 10^{-8}$ hour $^{-1}$, $\alpha_{bc} = 7 \times 10^{-9}$ hour $^{-1}$, $\alpha_{sul} = 3 \times 10^{-9}$ hour $^{-1}$, $M_{\min} = 5.236 \times 10^{-22}$ g, $M_{\max} = 5.236 \times 10^{-7}$ g.

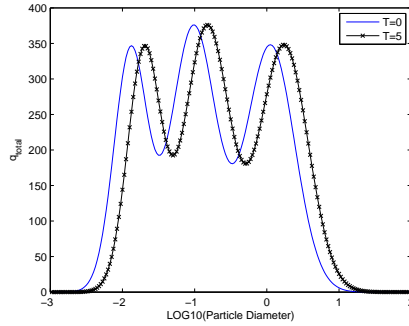


FIGURE 6. Initial distribution and numerical solution of the total mass concentration at time $T = 5$ hour for the problem.

of the total mass, we can see that the peak values keep almost unchanged. Table 4 gives Comparison of errors and ratios in time step by our method and the S-C-FEM scheme. It is obvious that our method has second-order accuracy in time step but the S-C-FEM only has first-order accuracy in time step.

5. Conclusion

In this work, an efficient time second-order characteristic finite element method was developed for solving the nonlinear multi-component aerosol dynamic equations on time and particle size. We proposed to use the highly accurate characteristic method to treat the advection-condensation/evaporation process and apply the high-order extrapolation along the characteristics to approximate the nonlinear coagulation terms. Theoretical analysis was given that the developed scheme was proved to be of second-order accuracy in time step. Numerical experiments on different multi-component aerosol dynamic problems were taken.

TABLE 4. Comparison of errors and ratios in time at $T = 5$ hours for the three-component aerosol condensation problem of aerosol water, black carbon and sulfate components with different Trimodal initial distributions by our method and the S-C-FEM scheme.

	Δt (hour)	$\frac{T}{4}$	$\frac{T}{8}$	$\frac{T}{16}$	$\frac{T}{32}$	$\frac{T}{48}$
Our method	E_∞	3.6334e-3	9.0022e-4	2.2148e-4	5.1539e-5	2.0771e-5
	Ratio	-	2.0130	2.0231	2.1035	2.2413
	E_2	3.4203e-3	8.4677e-4	2.0940e-4	5.0473e-5	2.1132e-5
	Ratio	-	2.0141	2.0157	2.0527	2.1473
S-C-FEM	E_∞	5.8231e-2	2.9768e-2	1.4421e-2	6.4375e-3	3.7271e-3
	Ratio	-	0.9680	1.0456	1.1636	1.3478
	E_2	5.4755e-2	2.7991e-2	1.3559e-2	6.0513e-3	3.5031e-3
	Ratio	-	0.9680	1.0457	1.1639	1.3481

References

- [1] I. J. Ackermann, H. Hass, M. Memmesheimer, A. Ebel, F. S. Binkowski, and U. Shankar, Modal aerosol dynamics model for Europe: Development and first applications, *Atmo. Envir.*, 1998 (32) 2981-2999.
- [2] P. G. Ciarlet, *The finite element method for elliptic problems*. Elsevier, 1978.
- [3] E. Debry and B. Sportisse, Solving aerosol coagulation with size-binning methods, *Appl. Numer. Math.*, 2007 (57) 1008-1020.
- [4] E. Debry, B. Sportisse and B. Jourdain, A stochastic approach for the numerical simulation of the general dynamics equation for aerosols, *J. Comput. Phys.*, 2003 (184) 649-669.
- [5] C. H. Jung, S. H. Park and Y. P. Kim, Size distribution of polydispersed aerosols during condensation in the continuum regime: Analytic approach using the lognormal moment method, *J. Aerosol Sci.*, 2006 (37) 1400-1406.
- [6] D. Katoshevski and J. H. Seinfeld, Analytical solution of the multicomponent aerosol general dynamic equation-without coagulation, *Aerosol Sci. Tech.*, 1997 (27) 541-549.
- [7] Y. P. Kim and J. H. Seinfeld, Simulation of multicomponent aerosol condensation by the moving sectional method, *J. Colloid Inter. Sci.*, 1990 (135) 185-199.
- [8] D. Liang, Q. Guo and S. Gong, A new splitting wavelet method for solving the general aerosol dynamics equation, *J. Aerosol Sci.*, 2008 (39) 467-487.
- [9] D. Liang, W. Wang and Y. Cheng, An efficient second-order characteristic finite element method for non-linear aerosol dynamic equations, *Internat. J. Numer. Methods Engng.*, 2009 (80) 338-354.
- [10] Z. Meng, D. Dabdub and J. H. Seinfeld, Size-resolved and chemically resolved model of atmospheric aerosol dynamics, *J. Geophys. Research: Atmospheres* (1984-2012), 103(D3):3419-3435, 1998.
- [11] C. Pilinis, Derivation and numerical solution of the species mass distribution equations for multicomponent particulate systems, *Atmospheric Environment. Part A. General Topics*, 1990 (4) 1923-1928.
- [12] S. E. Pratsinis, Simultaneous nucleation, condensation, and coagulation in aerosol reactors, *J. Colloid Inter. Sci.*, 1988 (124) 416-427.
- [13] A. Sandu and C. Borden, A framework for the numerical treatment of aerosol dynamics, *Appl. Numer. Math.*, 2003 (45) 475-497.
- [14] A. Sandu, W. Liao, G. R. Carmichael, D. K. Henze and J. H. Seinfeld, Inverse modeling of aerosol dynamics using adjoints: Theoretical and numerical considerations, *Aerosol Sci. Tech.*, 2005 (39) 677-694.
- [15] A. S. Wexler, F. W. Lurmann and J. H. Seinfeld, Modelling urban and regional aerosols-I. Model development, *Atmospheric Environment*, 1994 (28) 531-546.
- [16] E. R. Whitby, P. H. McMurry, U. Shankar and F. S. Binkowski, Modal aerosol dynamics modeling (No. PB-91-161729/XAB), Computer Sciences Corp., Research Triangle Park, NC (USA), 1991.

Department of Mathematics and Statistics, York University, Toronto, Ontario, M3J 1P3,
Canada

E-mail: kfu@mathstat.yorku.ca

Department of Mathematics and Statistics, York University, Toronto, Ontario, M3J 1P3,
Canada, and School of Mathematics, Shandong University, Jinan, Shandong, 250100, China

E-mail: dliang@mathstat.yorku.ca

School of Mathematics, Shandong University, Jinan, Shandong, 250100, China

E-mail: wangwq@sdu.edu.cn

College of Applied Sciences, Beijing University of Technology, Beijing, 100124, China

E-mail: mingcui@bjut.edu.cn